NANO LETTERS

2001
Vol. 1, No. 2
75−79

Lithium Doping of Multiwalled Carbon Nanotubes Produced by Catalytic Decomposition

G. Maurin,[†] F. Henn,*[,†] B. Simon,[‡] J.-F. Colomer,[§,||] and J. B. Nagy[§]

LPMC-UMR 5617 CNRS, University of Montpellier II Sciences and Techniques du Languedoc, cc 003, Pl. E. Bataillon, F-34095 Montpellier Cedex 05, France, SAFT, Direction de la Recherche, 111 Boulevard A. Daney, 33074 Bordeaux Cedex, France, LRMN, FUNDP, 61 rue de Bruxelles, B-5000 Namur, Belgium, and EMAT, University of Antwerpen (RUCA), Groenenborgerlaan 171 B-2020 Antwerpen, Belgium

Received October 26, 2000

ABSTRACT

Electrochemical lithium doping into carbon electrodes consisting of multiwalled carbon nanotubes produced by catalytic decomposition of acetylene has been carried out in button cells. Direct observation of the sample by low- and high-resolution transmission electron microscopy reveals that the lithium species are not intercalated between the graphene shells of nanotubes and that the electrochemical process is reversible. ^{7}Li NMR and Raman spectroscopies allow us to study the nature of interactions between lithium atoms and the host material and to propose an insertion mechanism that only implies a storage of lithium at the surface of nanotubes.

Since Iijima's discovery,[1] the carbon nanotubes generated tremendous interest. At the beginning, the quantity of carbon nanotubes available for experiments was very low, since the arc discharge method produced only small amounts and impure sample. During the last years, new methods as the catalytic vapor deposition[2,3] were developed and yielded multiwalled carbon nanotubes (MWNTs) in large scale and high purity. According to the "Russian Doll" model,[4,5] MWNTs are composed of graphene shells rolled into closed concentric cylinders with diameters on the order of nanometers and lengths of micrometers. Numerous attempts were then performed to fill them with various chemical species. Some studies involving their potential applications for the electrochemical storage of energy were reported.[6−8] The electrochemical results show that lithium redox reaction did occur in MWNTs and that the reversible capacity, depending on the processing condition, is in the range 100−400 Ah kg^{-1}. Furthermore, we have previously shown[8] that the intercalation of lithium into the structure of MWNTs (produced by the electric arc technique) proceeds through the graphene walls via structural defects. This intercalation led us to observe what we named a "necklace" structure. Moreover, electrochemical insertion of single-walled carbon nanotubes (SWNTs) has recently been reported.[9,10] It has been shown that lithium can be reversibly inserted into SWNTs and this electrochemical process induces structural disorder in SWNTs bundles. Compositions ranging from $Li_{1.7}C_6$ to $Li_{2.7}C_6$ after ball-milling (1000 Ah kg^{-1}) can be reached and are higher than the LiC_6 ideal value for graphite. Here, we report the electrochemical lithium doping of MWNTs produced by catalytic decomposition of acetylene at 600 °C. The aim of this work is to elucidate the mechanism of lithium insertion into this kind of MWNT and then to gain a better understanding of the relationship between the morphologies of the tubes that depend on the synthesis route and the insertion mechanism.

The material used in this investigation was multiwalled carbon nanotubes (MWNTs) produced by catalytic decomposition of acetylene at 600 °C over supported catalyst Co/zeolite NaY containing about 2.5 wt % metal. The details of the various steps of synthesis and purification were reported elsewhere.[3] The carbon nanotubes obtained were sinuous and entangled, their length can reach 10 μm, and their outer diameter ranged from 15 to 25 nm. The purity of the studied sample, estimated from random sampling and repeated scanning electron microscopy observations was as high as 90% (vol %).

The electrochemical lithium doping was carried out in Li/electrolyte/MWNTs button cells assembled in an argon-filled glovebox. Carbon nanotubes were used as the cathode, and lithium metal foil, as anode. The cathode was prepared by

* To whom correspondence should be addressed. E-mail: fegh@lpmc.univ-montp2.fr. Phone: +33 4 67 14 48 55. Fax: +33 4 67 14 42 90.
[†] University of Montpellier II.
[‡] Direction de la Recherche.
[§] FUNDP.
[||] University of Antwerpen.

10.1021/nl005517n CCC: $20.00
Published on Web 01/23/2001

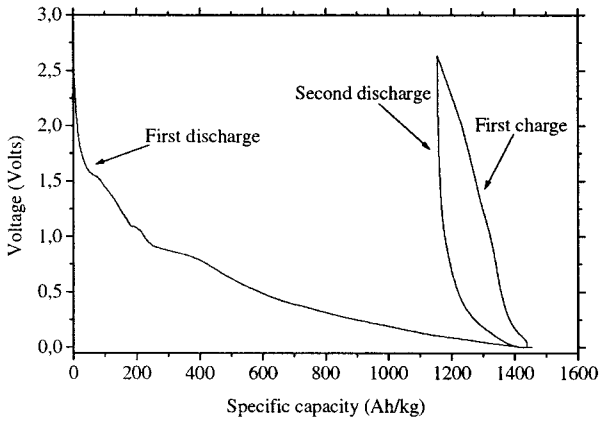

Figure 1. Typical cycling of a Li/$LiPF_6$/MWNTs cell at $I = 10$ mA/g. The voltage of the carbon electrode is measured vs the Li metal foil electrode.

mixing carbon nanotubes with 5% poly(tetrafluoroethylene) (PTFE) as a binder and 5% black carbon. The electrolyte was 1 M $LiPF_6$ dissolved in carbonate mixture EC/PC/3DMC. Cells were tested using a multichannel galvanostatic/potentiostatic system (Mac Pile). Several discharge/charge cycles were recorded with currents ranging from 5 to 10 mA per gram of carbon material. Figure 1 shows a typical discharge−charge curve of carbon nanotubes for the electrode technologies used. The open circuit voltage of about 10 button cells measured before the experiment was 2.7 V. This high value is due to the presence of carboxyl, carbonyl and hydroxyl groups, which are introduced during oxidative treatment and which covered the surface of the nanotubes. These groups functionalize the tubes[11] and usually increase the chemical reactivity of the material. This sample exhibits a reversible capacity of 300 Ah kg^{-1}, in the 0−2.7 V potential range, which is close to those obtained for graphite.[12] This capacity decreases slowly upon cycling and equals 260 Ah kg^{-1} after 20 cycles. The irreversible capacity (defined as the capacity difference between the first and second discharge) equals 1150 Ah kg^{-1} and is connected to the reduction of oxygenated species at the surface of the tubes and the formation of a passive protective layer occurring around 0.8 V consecutive to the decomposition of electrolyte. This capacity is related to the high surface area of the MWNTs, which is 265 m^2/g. In contrast to graphite,[12] where the successive steps of intercalation are characterized by voltage plateaus, or to MWNTs produced by the electric arc technique,[8] which exhibit a low-voltage pseudoplateau around 0.1 V, the voltage profile consists only of a decay zone from 2.7 to 0.0 V against the lithium metal foil electrode, as was usually observed for disordered carbons.[13] This different behavior seems to indicate that the lithium atoms are not intercalated between the pseudographitic layers. This observation is confirmed by X-ray diffraction, which indicates no modification of the inter-shell spacing for the lithiated sample. Consequently, the insertion mechanism differs with the nature of the studied MWNTs.

Moreover, the voltage curve for the studied MWNTs exhibits a large hysteresis in the discharge/charge profile (Figure 2a). The difference observed between the potential of lithium doping and dedoping potential reinforces the argument that lithium ions are not intercalated between the graphene shells, because, in this case, the two processes would perform with a low-voltage difference, as is the case for MWNTs produced by the electric arc technique (Figure 2b),[8] but rather are trapped in structural defects at the surface of the tubes or in cavities created by the entanglements of the tubes. This observed hysteresis can be explained by the chemical interactions between lithium species and functional groups, these electrostatic interactions, namely $-CO^-Li^+$, needing higher voltage for removing lithium from the carbon nanotubes.

Morphologies and structures of these samples were studied by using JEOL EX2 and JEOL 200 CX instruments (TEM low and high resolution). Figure 3a shows a typical TEM overall image of the pristine MWNTs that are entangled, and a HRTEM picture of one of them (Figure 3b) underlines that the carbon layers are perfectly parallel to the tube axis. Figure 3c is a TEM picture of the delithiated sample. The general aspect of the tubes seems to be unchanged after dedoping. The tubular morphology remains intact, and this observation indicates that the insertion process seems to be reversible. Figure 3d presents an HRTEM picture of MWNTs after dedoping. The organization of the carbon layers appears

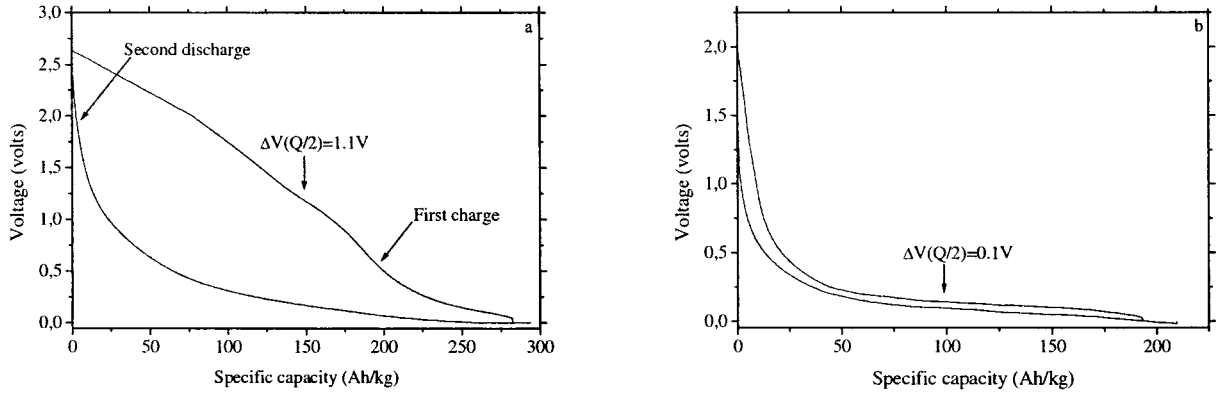

Figure 2. (a) Large hysteresis in the second discharge/first charge profile for MWNTs produced by catalytic decomposition. The difference between the potential of lithium dedoping and doping potential for the half reversible capacity ($\Delta V(Q/2)$) is very high and equals 1.1 V. (b) Second discharge/first charge curve for MWNTs produced by the electric arc technique exhibits a low $\Delta V(Q/2)$ of 0.1 V.

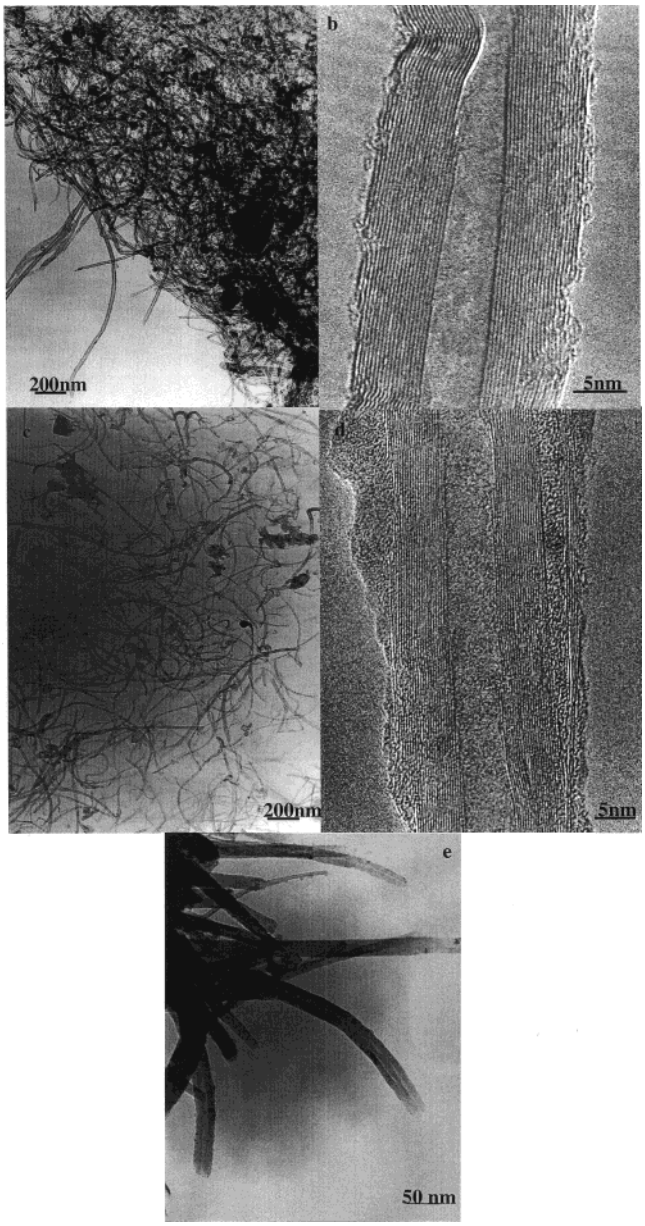

Figure 3. (a) Typical transmission electron microscopy (TEM) views of entangled catalytic MWNTs. (b) HRTEM image of pristine tube with carbon layers parallel to the tube axis and with clean outer surface. (c) TEM image of the nanotubes after the dedoping process. (d) HRTEM picture of a delithiated nanotube. (e) TEM view of lithiated nanotubes.

unchanged, and some parts of the tube are covered by a thin film of carbon species, which could be the passive layer or the damaged outer carbon layers. Finally, Figure 3e presents the TEM image of lithiated nanotubes. We notice that the tubes keep their initial shape and that their diameter remains almost constant. This observation indicates that the lithium species do not penetrate the graphene layers, as was the case for intercalated MWNTs produced by the electric arc technique,[8] where the so-obtained "necklace" structure consists of a heterogeneous intercalation of lithium between the graphene layers. The TEM picture shows that the lithium doping is only limited at the surface of the tubes: these ions do not cross the outer graphene wall despite the high concentration of lateral defects. The outer surface of the lithiated tubes is covered by a thin film of lithium species such as Li_2CO_3. This phenomenon could be explained by considering the presence of numerous functional groups at the outer surface of the tubes. These groups react with the lithium ions and prevent them from reaching the graphene layers from the side of the tubes.

High-resolution magic angle spinning (HRMAS) ^{7}Li NMR was conducted with a Bruker ASX 400 spectrometer operating at a ^{7}Li resonance frequency of 116 MHz. The HRMAS ^{7}Li spectrum of the lithiated sample is displayed in Figure 4. It exhibits a broad band centered around 0 ppm. This band can be separated into two: one is a narrow band with resonance frequency of -0.8 ppm, and the other one is a broad band with a resonance frequency shift of -0.1 ppm. The first one localized at -0.8 ppm is also present in the spectrum obtained for the totally delithiated sample. Therefore, this signal can be assigned to the solid electrolyte interphase (SEI), which consists of one or more ionic lithium compounds such as Li_2CO_3, and to the remaining electrolyte.[14] The broad band at -0.1 ppm is often observed in lithiated disordered carbons and is a subject of controversy in the literature. Sato et al.[15] propose a Li_2 molecule model, Zheng et al.[16] suggest that lithium may be bound somehow in the vicinity of the hydrogen atoms, and insertion can be envisaged either at the surface of the microcrystallites composed of several carbon sheets or in their microcavities[17] or at the edges of graphene layers.[18] In our case, we can assign it to ionic lithium stored in reversible sites as defects at the surface of the carbon nanotubes, as was observed previously in disordered carbons.[19,20] This result is different from those obtained for the previously studied MWNTs,[8] where a Knight shift at 43 ppm characterized intercalated species residing between graphene shells. This technique confirms the different insertion mechanism of lithium in our sample where only adsorption at the surface can be reached.

Micro-Raman spectra were recorded using a Labram spectrometer coupled to a 13 × 40 Olympus microscope equipped with a 100× objective. Raman spectra were obtained at ambient temperature with the 632.8 nm radiation from a helium neon laser. Figure 5a shows first-order micro-Raman spectrum of pristine carbon nanotubes. The main Raman lines observed are at 1578 and 1328 cm^{-1}. The band centered around 1578 cm^{-1} corresponds to the G mode representing the movement in opposite directions of two neighboring carbon atoms in a graphene sheet.[21] The 1328 cm^{-1} band, assigned to the D_1 mode, is attributed to defects in the curved graphene sheet, tube ends, and staging disorder.[22] An additional Raman line at 1610 cm^{-1} (called D_2 mode) is mainly due to structural defects. The $R_1 = A_{D1}/A_{G1}$ and $R_2 = A_{D2}/A_{G2}$ ratios, where A corresponds to the area of the Lorentzian functions, allow us to estimate the extents of structural defects. In this case, these ratios are 1.9 and 0.3, respectively. The micro-Raman spectrum of the delithiated sample (Figure 5b) is similar to those obtained for the pristine material. The low modification of the R_1 and R_2 ratios reveals that the concentration of structural defects is likely to remain almost constant. These observations

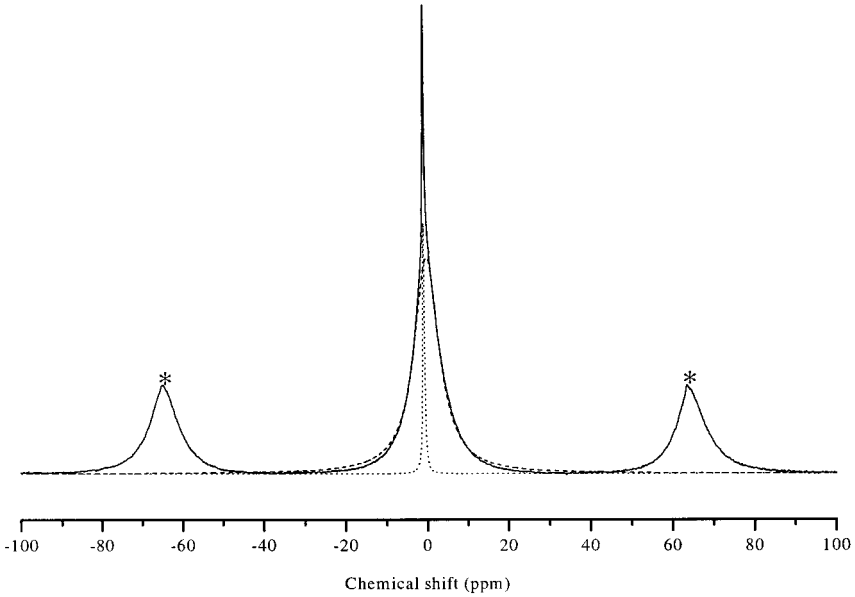

Figure 4. High resolution ^{7}Li NMR spectrum of the lithiated sample. The spin frequency is equal to 13 kHz. The peaks denoted by * are "spinning sidebands" and can be distinguished from the central peaks by changing the spin frequency.

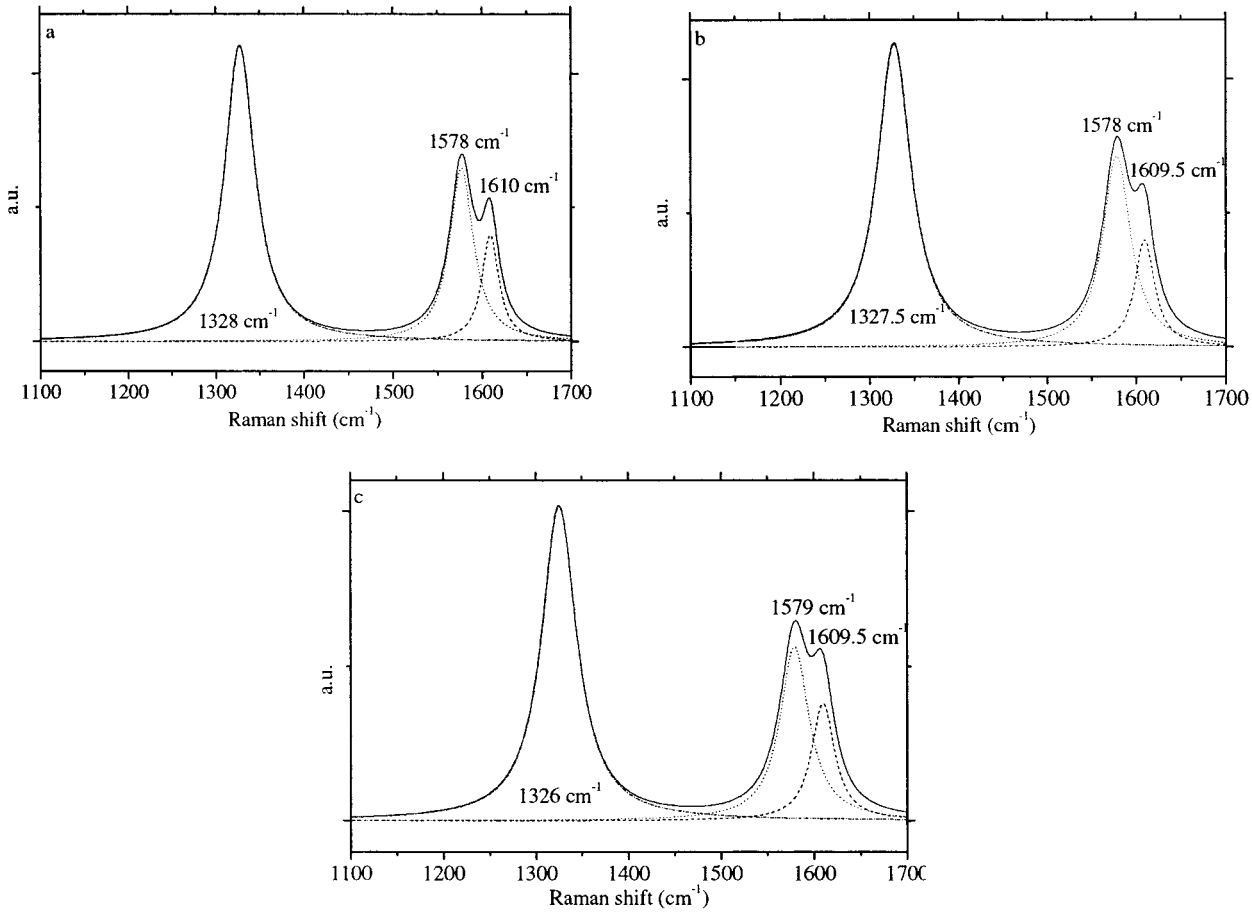

Figure 5. First-order Raman spectra: (a) pristine material; (b) delithiated sample; (c) lithiated sample. The various spectra are fitted by Lorentzian functions that are attributed to D_1, D_2, and G bands, respectively.

confirm that the structure of nanotubes is only slightly modified during the dedoping process. Figure 5c presents the micro-Raman spectrum of the lithiated sample. If the lithium was inserted between graphene layers of the tubes, it would affect the electronic structure of the organized layers and the peak number of the G band would be changed.[23,24] However, the spectrum exhibits no change in the peak frequency. This behavior is similar to those obtained for

mesocarbons heat treated at 700 °C[25,26] and have been attributed to lithium insertion into regions without organized graphitic structure. This result seems to confirm the hypothesis that lithium species only trapped at the surface of nanotubes may be within cavities generated by structural defects or entanglements. In this paper and in comparison with the data we have recently published,[8] we show that the insertion mechanism of lithium in MWNTs depends on their structural characteristics and their chemical composition, which can be modified by the means of synthesis and by chemical treatment. In contrast to MWNTs produced by the electric arc technique where lithium species cross the side of the tubes and reach the graphene layers, the functional groups present at the surface of the catalytic-MWNTs prevent this kind of diffusion. Then, the lithium species are only stored at the surface of the tubes, maybe in cavities.

Acknowledgment. HREM work has been performed at EMAT-Antwerp (within the framework of IUAP-PAI 4/10).

References

(1) Iijima, S. *Nature* (London) **1991**, *354*, 56.
(2) Hamwi, A.; Alvergnat, H.; Bonnamy, S.; Beguin, F. *Carbon* **1997**, *35* (6), 723.
(3) Colomer, J. F.; Piedigrosso, P.; Willens, I.; Journet, C.; Bernier, P.; Van Tendeloo, G.; Fonseca, A.; Nagy, J. B. *J. Chem. Soc., Faraday Trans*. **1998**, *94*, 3753.
(4) Ebessen, T. W.; Ajayan, P. M. *Nature* (London) **1992**, *358*, 220.
(5) Guerret-Piecourt, C.; LeBouar, Y.; Loiseau, A.; Pascard, H. *Nature* **1994**, *372*, 761.
(6) Che, G.; Lakshmi, B. B.; Fisher, E. R.; Martin, C. R. *Nature* (London) **1998**, *393*, 346.
(7) Frackowiak, E.; Gautier, S.; Gaucher, H.; Bonnamy, S.; Beguin, F. *Carbon* **1999**, *37*, 61.
(8) Maurin, G.; Bousquet, C.; Henn, F.; Simon, B.; Bernier, P.; Almairac, R. *Chem. Phys. Lett*. **1999**, *312*, 14.
(9) Gao, B.; Bower, C.; Lorentzen, J. D.; Fleming, L.; Kleinhammes, A.; Tang, X. P.; Mc. Neil, L. E.; Wu, Y.; Zhou, O. *Chem. Phys. Lett*. **2000**, *327*, 69.
(10) Claye, A.; Lee, R.; Benes, Z.; Fischer, J. *J. Electrochem. Soc*. **2000**, *147*, 8 2845.
(11) Tsang, S. C.; Chen, Y. K.; Harris, P. J. F.; Green, M. L. H. *Nature* **1994**, *372*, 159.
(12) Dahn, J. R. *Phys. Rev. B* **1991**, *44 (17)*, 9170.
(13) Takami, N.; Satoh, A.; Ohsaki, T.; Kanda, M. *Electrochim. Acta* **1997**, *42* (16), 2537.
(14) Nakagawa, Y.; Wang, S.; Matsumura, Y.; Yamaguchi, C. *Synth. Met.* **1997**, *85*, 1363.
(15) Sato, K.; Noguchi, M.; Demachi, A.; Oki, N.; Endo, M. *Science* **1994**, *264*, 556.
(16) Zheng, T. McKinnon, W. R.; Dahn, J. R. *J. Electrochem. Soc*. **1996**, *143* (7), 2137.
(17) Mori, Y.; Iriyama, T.; Hashimoto, T.; Yamazaki, S.; Kawakami, F.; Shiroki, H.; Yamabe, T. *J. Power Sources* **1995**, *56*, 205.
(18) Xiang, H. Q.; Fang, S. B.; Jiang, Y. Y. *J. Electrochem. Soc*. **1997**, *144*, L187.
(19) Takami, N.; Satoh, A.; Oguchi, M.; Sasaki, H.; Ohsaki, T. *J. Power Sources* **1997**, *68*, 283.
(20) Guerin, K.; Menetrier, M.; Fevrier-Bouvier, A.; Flandrois, S.; Simon, B.; Biensan, P. *Solid State Ionics* **2000**, *127*, 187.
(21) Hiura, H.; Ebbesen, T. W.; Tanigaki, K.; Takahashi, H. *Chem. Phys. Lett*. **1993**, *202*, 509.
(22) Bacsa, W. S.; Ugarte, D.; Chatelain, A.; De Heer, W. A. *Phys. Rev. B* **1994**, *50*, 15473.
(23) Inaba, M.; Yoshida, H.; Ogumi, Z.; Abe, T.; Mizutani, Y.; Asano, M. *J. Electrochem. Soc*. **1995**, *142 (1)*, 20.
(24) Maurin, G.; Bousquet, C.; Henn, F.; Simon, B.; Almairac, R.; Bernier, P. *Solid State Ionics* **2000**, *136−137*, 1295.
(25) Inaba, M.; Yoshida, H.; Ogumi, Z. *J. Electrochem. Soc*. **1996**, *143 (8)*, 2572.
(26) Endo, M.; Kim, C.; Karaki, T.; Fujino, T.; Matthews, M. J.; Brown, S. D. M.; Dresslhaus, M. S. *Synth. Met.* **1998**, *98 (1)*, 17.

NL005517N